

Negative Contrast Enhancement in T₂*-weighted Images of the Human Brain During Hyperoxia

D. T. Pilkinton¹, S. Gaddam¹, M. A. Elliott¹, and R. Reddy¹

¹Center for Magnetic Resonance and Optical Imaging, University of Pennsylvania, Philadelphia, PA, United States

Introduction

Studies have shown that increasing the inspired fraction of oxygen ($\text{FiO}_2 > 0.21$) produces positive contrast enhancement in T₂*-weighted images in brain tissue based on the increase blood oxygenation and subsequent decrease in venous concentration of deoxyhemoglobin, which is paramagnetic [1],[2]. Hyperoxic contrast has been used to calculate cerebral blood volume [2] and to standardize signal changes in BOLD fMRI experiments [3]. The increase in venous blood oxygenation is due to excess dissolved oxygen carried in the plasma of arterial blood, which during hyperoxia contains completely saturated hemoglobin. While it is known that molecular oxygen is paramagnetic and that increased concentrations significantly reduce T₁, the effect in heavily T₂*-weighted images is generally considered to be negligible when compared to the effects of BOLD contrast, especially at low FiO_2 levels [2]. Here we show using hyperoxic contrast in a whole brain EPI study at 3T that, although positive contrast enhancement dominates most regions, the inferior regions of the brain show significant negative contrast enhancement in strongly T₂*-weighted images, even at low oxygen concentration ($\text{FiO}_2 < 0.6$). These regions have a relatively high fraction of arterial cerebral blood volume, since they contain large arteries that feed the brain. We hypothesize that this negative contrast is due to the shortening of T₂* in arterial blood due excess paramagnetic molecular oxygen dissolved in the plasma.

Materials and Methods

A single male subject was imaged under a protocol approved by our Institutional Review Board. The subject first breathed medical air followed by 100% oxygen at 15L/min from nasal cannula (generally accepted to be less than $\text{FiO}_2 < 0.6$, due to the entrainment of room air) during six alternating epochs lasting approximately five minutes each. All images were acquired on Siemens Trio 3T, using a vendor-supplied 8-channel receiver head coil. A standard EPI sequence was used with TE/TR: 34/4500ms, FOV: 256x256, 64 phase encodes, 24 slices with 6mm thickness with a 1.25mm separation (nominal resolution of 4x4x6mm). Sixty full volume acquisitions were acquired during each epoch. Also, two structural images were obtained: (1) a product-standard T1-weighted structural 3D MPRAGE was taken with TI: 1100ms, 256 phase encodes (partial-Fourier reduced to 192), 96 slice encodes, FOV: 256x256x192 (nominal resolution of 1x1x2mm) and (2) a proton-density weighted 2D GRE with TE/TR: 5.2ms/271ms, 256 phase encodes, FOV: 256x256, 24 slices with 6mm thickness (nominal resolution of 1x1x6mm).

Prior to the final analysis, the images were brain-extracted, motion-corrected, high-pass filtered to remove long-term signal drift, and spatially-smoothed with a 4x4x4mm kernel using FSL Tools [4]. Signal intensities were analyzed by taking the median of the three baseline (air-breathing) epochs and subtracting from and dividing by the median three hyperoxic epochs to produce percent signal change from baseline during hyperoxia.

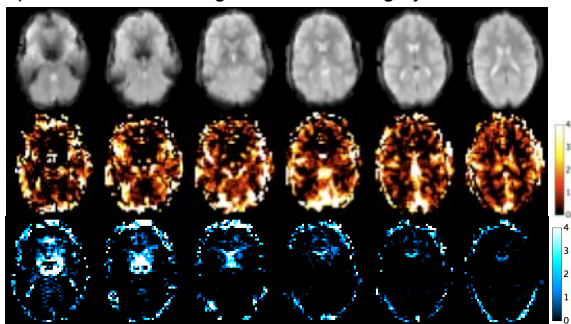


Fig. 1. Magnitude EPI images (top), percent positive (middle), and percent negative signal change (bottom) during oxygen breathing.

Images were then compared using the same color mapping scheme for negative and positive contrast enhancement. In an effort to better resolve the EPI data, it was registered to the structural data sets using a twelve degree-of-freedom affine matrix registration algorithm, FLIRT, which is part of FSL tools. In this process the EPI data is up-sampled to the resolution of the MPRAGE data. This allowed for the location of arteries and veins in the EPI images by a voxel-wise comparison to the structural data.

Results

Fig. 1 shows the magnitude EPI images (top row), percent positive (middle row), and percent negative signal change (bottom row) that occurred during oxygen breathing. The signals were taken as the average signal intensity during the equilibrium or plateau region of the signal curves (the first twelve acquisitions during each epoch were discarded). Fig. 2 shows the result of the registration the EPI data to the structural data. The images and signal curves correspond across the row; the voxels at the arrows represent an artery, internal carotid artery, and vein, inferior sagittal sinus located on the structural images. The curves to the right show percent signal change between the plateau to inhalation of 15L/min oxygen by nasal cannula as indicated by the blue boxes.

Discussion

The study demonstrates that although positive contrast enhancement dominates most brain regions, there are large regions at the inferior end of the brain that produce substantial negative contrast in strongly T₂*-weighted images, even with the relatively low FiO_2 levels associated with moderate flow nasal cannula. We believe that this negative contrast is associated with paramagnetic oxygen dissolved in the plasma of arterial blood. This idea is strongly supported by the data in Fig. 2; signal in voxels associated with arteries show clear negative contrast enhancement modulated by the hyperoxic contrast, as opposed to the positive contrast in voxels associated with veins. Techniques that assume that positive contrast enhancement dominates, such as CBV calculations [2], are likely to be confounded by these negative signal changes in regions like these.

On the other hand, we believe that this effect can also be exploited to provide useful additional information for this experiment. In particular, it can provide the temporal resolution necessary to dynamically measure the arterial input of hyperoxic contrast being delivered to tissues. The arterial input function to the tissue can be measured, allowing accurate dynamic measurements to be made. This is currently the focus of ongoing work.

References

[1] Losert, et al. *Magn. Reson. Med.* (2002); [2] Bulte, et al. *J. Magn. Reson. Imag.* (2007); [3] Chiarelli, et al. *Neuroimage* (2007); [4] Smith, et al.. *Neuroimage* (2004).

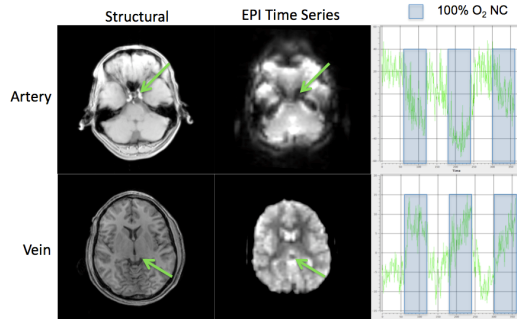


Fig. 2. EPI data registered to the structural data. The green arrows show the internal carotid artery (top) and inferior sagittal sinus (bottom), with the associated voxel signal time (right).